

Time-Frequency Representation For Estimating Young's Modulus and Poisson's Ratio Of Materials

Abdelkader Elhanaoui¹, Elhoucein Aassif¹, Gérard Maze², Dominique Décultot²

¹LMTI, Ibn Zohr University, Faculty of Sciences, BP 8106
Agadir 80000, Morocco

²LOMC UMR CNRS 6294, Normandie Université,
75 rue Bellot, CS 80 540, Le Havre University,
76058 Le Havre, France

ABSTRACT:

The present paper examines a new procedure for estimating Young's modulus and Poisson's ratio of homogeneous materials constituting the one-layer thin tubes. The work is done from the use of the time-frequency representation. Spectrogram and its reassigned version have been chosen to analyze experimentally acoustic signals backscattered by air-filled tubes immersed in water. For reduced frequencies ranging from 0.1 to 500, time-frequency images have shown the presence of the Symmetrical and the Antisymmetrical waves. Satisfactory resolution and good localization in the time-frequency plane have been observed in the case of concentrated spectrogram. Reduced cutoff frequencies of A_1 and S_1 waves have also been extracted from Spectrogram and concentrated Spectrogram time-frequency images. A good agreement has, therefore, been observed. Comparisons with results obtained by experiment indicate that mechanical parameters such as Young's modulus and Poisson's ratio of aluminum and copper are evaluated accurately.

Keywords: Young's modulus; Isotropic elasticity; Acoustic scattering; one-layer cylindrical tube; Time-frequency representation; Proper modes theory.

I. INTRODUCTION

The guided waves become in recent years an important tool in non-destructive characterization and have been utilized in many applications [1-11]. The longitudinal and the transversal waves in structures are the main choice for computation of the elastic deformation characteristics. However, relatively few studies have focused on mechanical / elastic properties of isotropic materials constituting plaques or circular cylindrical thin tubes, using the time-frequency representation (TFR). In this paper, we aim to measure the mechanical parameters of air-filled thin tubes immersed in water. The time-frequency representation, which is essentially an energy distribution in the time- frequency (t,v) plane, has proven to be an effective tool for analyzing the non-stationary signals [12-13]. The most popular analysis tools in many cases are the spectrogram and Wigner-Ville [14- 15]. This work presents the application of Spectrogram (Sp) and concentrated spectrogram (CSp) to study acoustic signals backscattered by thin aluminum and copper tubes of inner over outer radii ratio denoted by b/a . CSp representation is motivated by a desire to get the best localization and resolution of the time-frequency analysis. Firstly; the

Spectrogram is applied for making a preparative time-frequency analysis. Then, CSp representation is used for a fine frequency resolution.

The organization of the paper is as follows; In Section I, we briefly describe the acquisition of experimental acoustic signals and give examples related to our study. In Section II, we introduce background of time-frequency representations. In Section III, we give the Hooke's law, and expressions of Young's modulus and Poisson's ratio parameters of homogeneous materials. In Section IV, we present the time-frequency images, and estimate in detail, Young's modulus and Poisson's ratio values of aluminum and copper. The results obtained are fully discussed. Finally, conclusion is given.

1. Backscattering by an air-filled thin tube

1.1. Experimental setup

The experimental system, shown in Fig. 1, is constituted of a pulse generator *Sofranel 5052PR*, a digital oscilloscope *LeCroy 9310M -300MHz*, a personal computer, a transducer and an air-filled tube immersed in water. The water density ρ_w is equal to $1g.cm^{-3}$. The acoustic velocity wave c_w , measured at

the ambient temperature 20°C , is equal to $1,470\text{ mm}\cdot\mu\text{s}^{-1}$. The broadband transducer of a 10MHz central frequency and a 10mm diameter, placed opposite of the tube, is utilized successively as

emitter and receiver. It is excited by a short pulse generated by the pulse generator. Samples used are thin aluminum and copper tubes. The inner over outer radius ratio b/a approaches 1.

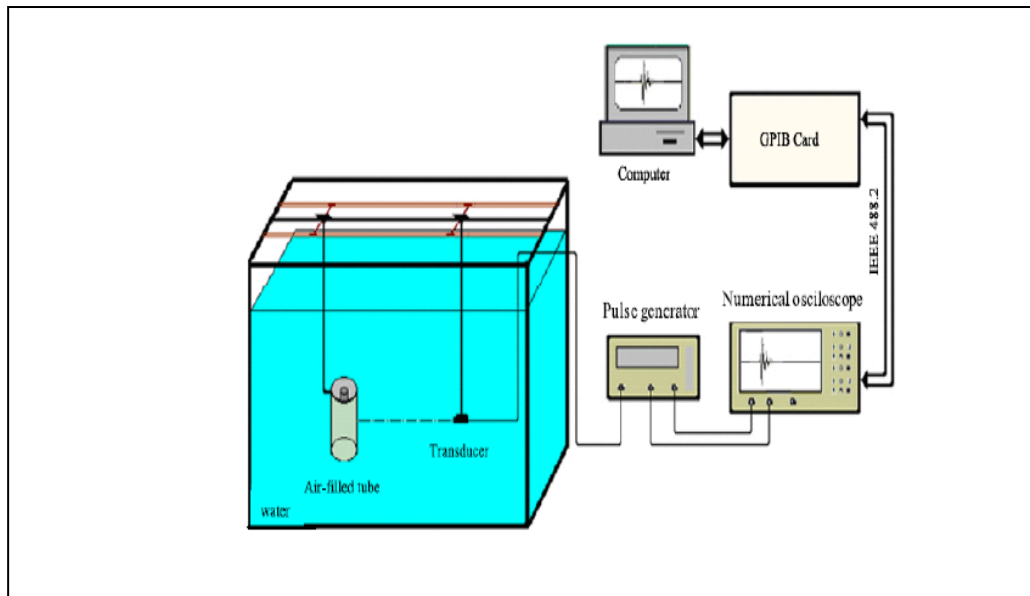
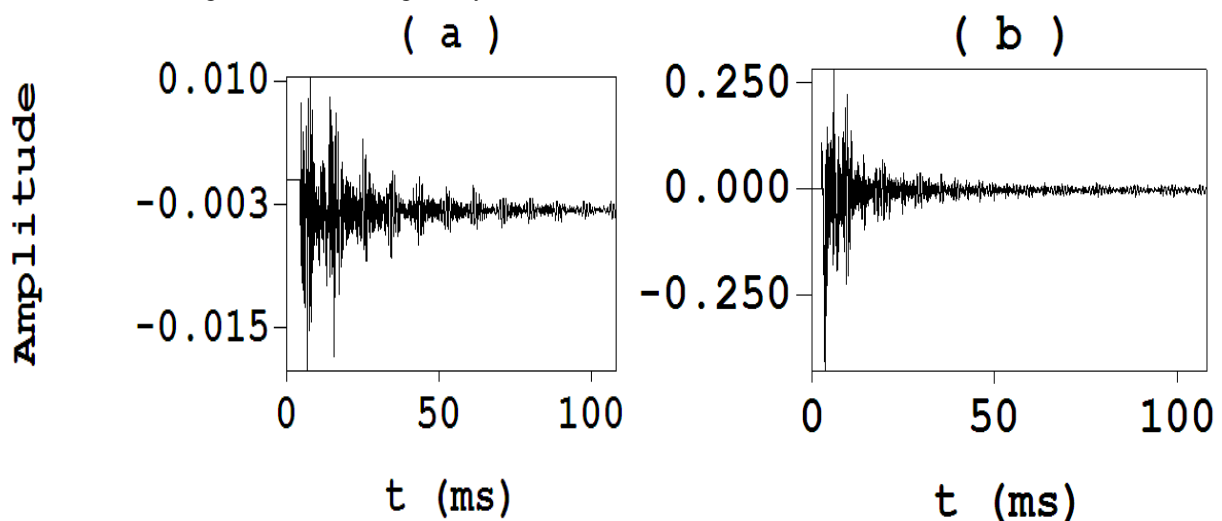


Figure 1. General geometry of backscattering by an-air filled tube immersed in water.

II. Experimental filtered signals for the studied shells

Fig.2 shows four examples of experimental signals backscattered by aluminum and copper tubes of inner over outer radii ratio equal to 0.90 , 0.95 , 0.93 and 0.94 respectively. The impulse responses are composed of a sequence of echoes that are related to guided waves propagating around circumferences of the targets. On the same figure, we can observe several waveform packets with low amplitude that are associated to the *A Scholte* wave and various guided waves designed by S_0 , A_1 , S_1 , etc.



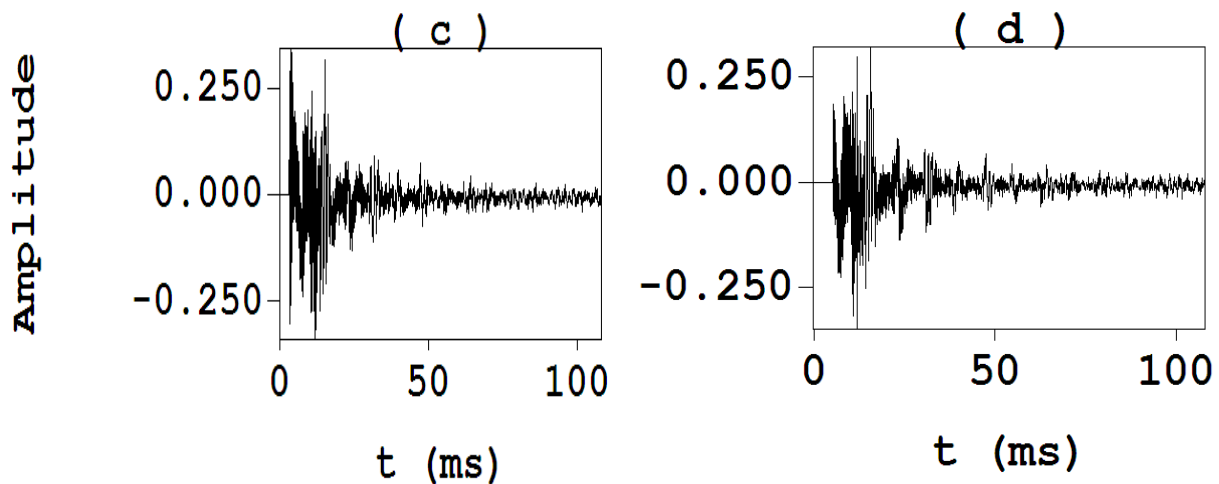


Fig. 2: Experimental signals backscattered by thin tubes: (a): aluminum 0.90 ; (b): aluminum 0.95; (c): copper 0.93 ; (d): copper 0.94.

III. SPECTROGRAM (SP) AND CONCENTRATED SPECTROGRAM (CSP)

SP and *CSP* representations are chosen to study acoustic signals backscattered by air-filled one-layer cylindrical tubes immersed in water [12-15]. *CSP* is motivated by many advantages, especially that it is linear; which simplifies the interpretation of the transform and has an inverse representation that ensures the possibility of the analyzed signal reconstruction [15-18].

1. Spectrogram

Short-time Fourier transform (*STFT*) is defined as [14],

$$STFT(l, k) = \sum s(l+m)h(m) \exp(i2\pi m(k/K - 1/2)) \quad (1)$$

Where s is the signal needed to analyze; $k=0,1,\dots,K-1$; $l=0,1,\dots,L-1$; $n=0,1,\dots,N-1$; M is the width of the window $h(m)$. L depends on the entire signal length N , and K is the length of the single running Discrete Fourier transform.

The energy of each *STFT* line is calculated as follows:

$$SP(l, k) = |STFT(l, k)|^2 \quad (2)$$

Theoretically, *SP* representation has a poor time-frequency resolution.

2. Reassigned Spectrogram

The computation of the time-frequency coordinates for each *STFT* line and the new locations are obtained by calculating local group delay as,

$$T(l, k) = \text{Arg}(STFT(l, k)STFT^*(l, k-1))K / (2\pi F_e) \quad (3)$$

And channelized instantaneous frequency as,

$$F(l, k) = \text{Arg}(STFT(l, k)STFT^*(l-1, k))F_e / (2\pi) \quad (4)$$

Where $STFT^*$ is the complex conjugate of *STFT* and *Arg* denotes the argument of a complex number, F_e marks sampling rate. Relocated coordinates are obtained by [15-18],

$$(t_l, \nu_k) \rightarrow (t_l - T(l, k), F(l, k))$$

t_l is the delay of l^{th} frame and ν_k is the frequency of center k^{th} channel.

The energy of each *STFT* line is determined by,

$$CSP(l, k) = |STFT(l, k)|^2 \quad (5)$$

IV. YOUNG'S MODULUS

1. Elastic constants

By The most general linear relationship which connects stress to strain is provided by the generalized version of the well-known Hooke's law [19],

$$\sigma = C.\varepsilon \quad (6)$$

In which σ denotes the stress tensor, ε the strain tensor and the elements of the fourth-order tensor C are the so-called elastic constants. The elastic constants are fundamental materials parameters providing detailed information on the mechanical properties of materials. The knowledge of these data may enable prediction of mechanical behavior in many different situations.

For an isotropic, homogeneous, linearly elastic material, the theory of elasticity demonstrates that it is possible to reduce the 21 components of the C tensor to two material constants (λ and μ) which are called the *Lamé* constants [19].

The phase velocities of the longitudinal and shear waves are respectively [20],

$$c_L = \sqrt{\frac{\lambda + 2\mu}{\rho}} \quad (7)$$

$$c_T = \sqrt{\frac{\mu}{\rho}} \quad (8)$$

Where ρ denotes the density; its values for aluminum and copper are equal to $2,800 \text{ g.cm}^{-3}$ and $8,920 \text{ g.cm}^{-3}$ successively.

Young's modulus and Poisson's ratio are expressed in function of the above quantities by [20],

$$E = \rho c_T^2 \frac{3c_L^2 - 4c_T^2}{c_L^2 - c_T^2} \quad (9)$$

$$\nu_p = \frac{c_L^2 - 2c_T^2}{2(c_L^2 - c_T^2)} \quad (10)$$

2. Case of a thin tube

At any given value of reduced frequency $x=2\pi\omega/c_w$, guided waves can be generated in the tube characterized by inner over outer radii ratio (b/a).

The phase velocity is directly related to the ratio b/a and the reduced cutoff frequency x_c as [21],

$$c_T = \frac{c_w}{\pi} \left(1 - \frac{b}{a}\right) x_c (A_1) \quad (11)$$

$$c_L = \frac{c_w}{\pi} \left(1 - \frac{b}{a}\right) x_c (S_1) \quad (12)$$

Where A_1 and S_1 are the antisymmetrical and the symmetrical waves respectively.

V. RESULTS AND DISCUSSIONS

1. Time-frequency images

SP and *CSP* given successively by the Eq. 2 and Eq. 5 are utilized in the work. Time- frequency images of the acoustic signal backscattered by aluminum and copper one-layer tubes are presented in Fig. 3 and Fig. 4. A_1 and S_1 waves are indicated in the above figures. Reduced cutoff frequencies for these mentioned waves are estimated by the asymptotic lines along the time axis, and presented in the table I.

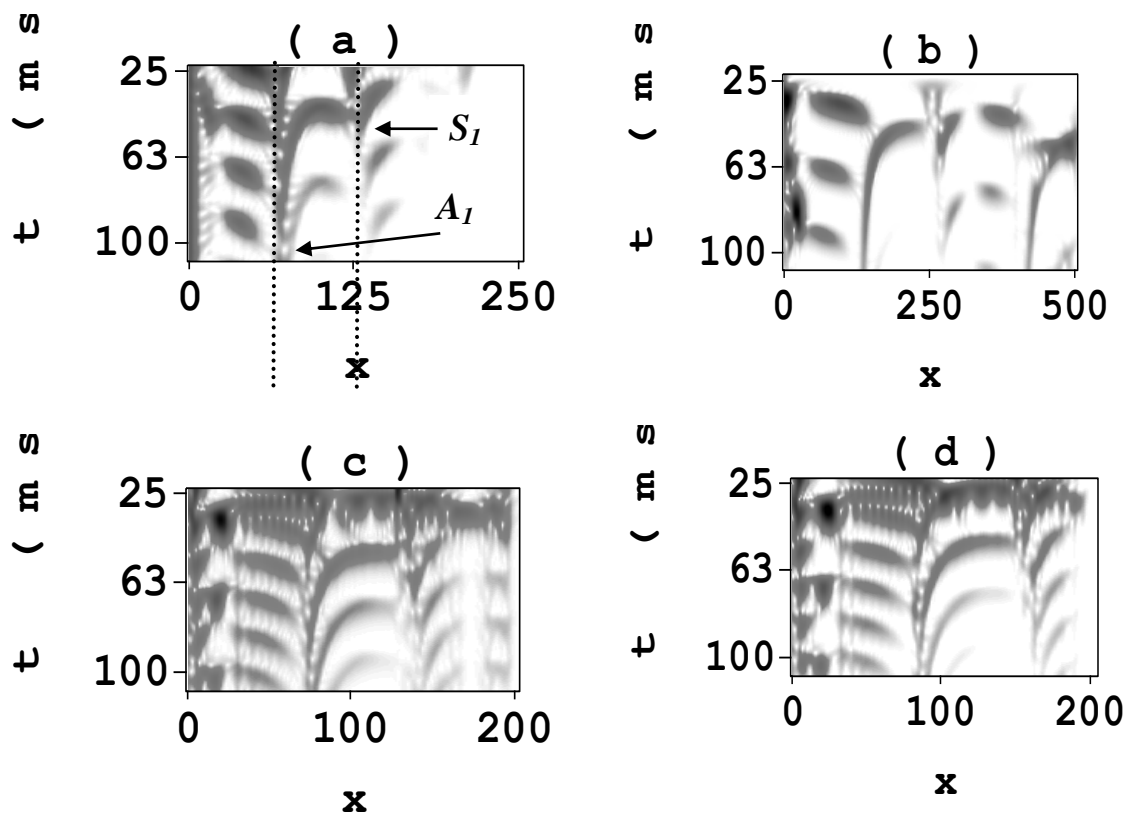
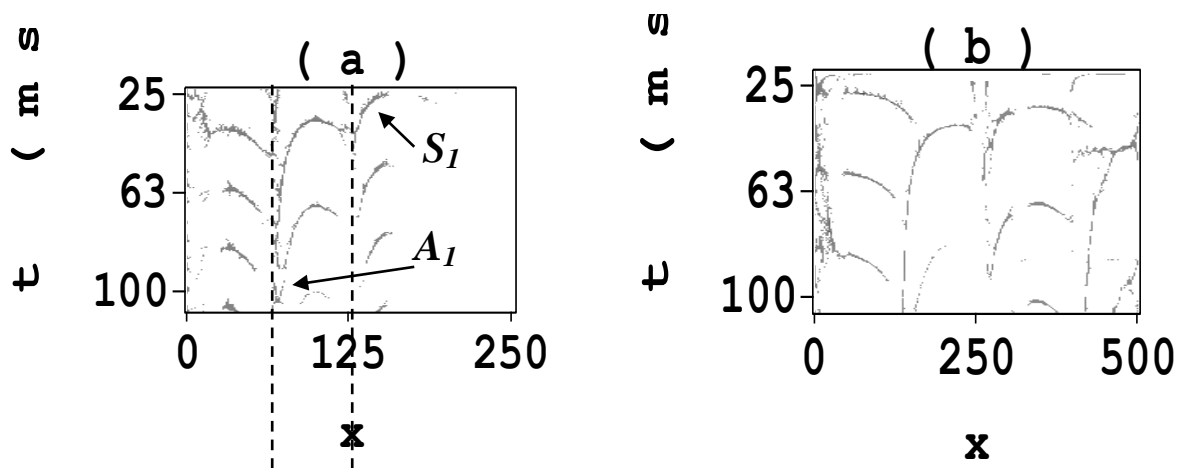


Fig. 3: Spectrogram images of experimental signals of Fig. 2 : (a): aluminum 0.90 ; (b): aluminum 0.95 ; (c): copper 0.93 and (d): copper 0.94.



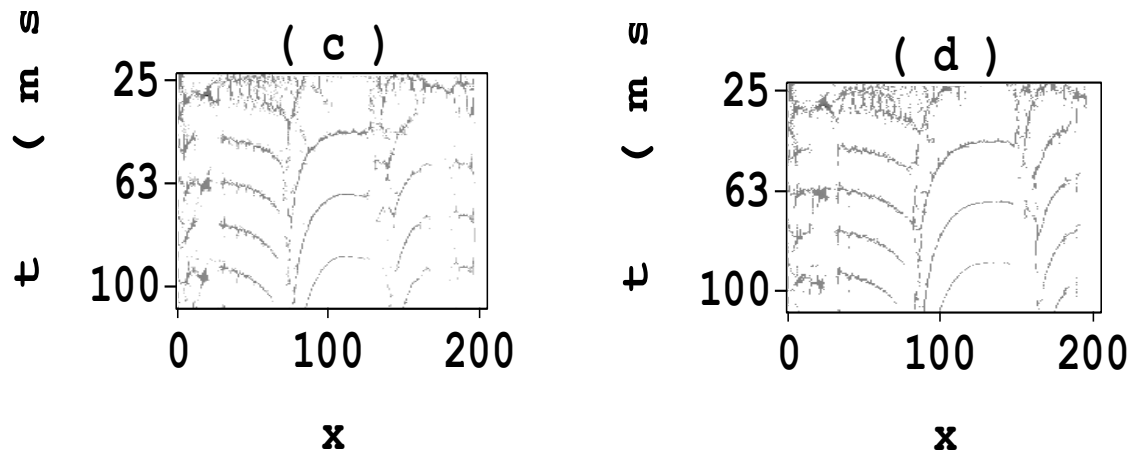


Fig. 4: Concentrated spectrogram images of experimental signals of Fig. 2 : (a): aluminum 0.90 ; (b): aluminum 0.95 ; (c): copper 0.93 and (d): copper 0.94.

Table I: Reduced cutoff frequency values of A_1 and S_1 waves

Guided waves	A_1 wave		S_1 wave	
	Spectrogram	Concentrated Spectrogram	Spectrogram	Concentrated Spectrogram
Aluminum ($b/a= 0,90$)	64,5	65	133	134,2
Aluminum ($b/a= 0,95$)	130	130,6	267,5	268
Copper ($b/a= 0,93$)	69,5	70,1	139,5	140
Copper ($b/a= 0,94$)	81,5	82,2	163	164

From Fig. (3), it is seen that the frequency resolution is affected.

From Fig. (4), it is found that time-frequency resolution is better when using *CSp*. It allows a better readability of guided waves that are propagated around each tube.

2. Estimation of Young's modulus and Poisson's ratio of aluminum and copper

In this paper, reduced cutoff frequencies for A_1 and S_1 waves are extracted in *SP* and *CSP* images. Then, the phase velocity of shear and longitudinal waves are rapidly evaluated, relatively to the aluminum and the copper, using Eq. (11) and Eq. (12); results are presented in Table II.

Table II: Phase velocities of shear and longitudinal waves ($\text{mm}.\mu\text{s}^{-1}$).

Phase velocities	c_T		c_L	
	Spectrogram	Concentrated Spectrogram	Spectrogram	Concentrated Spectrogram
Aluminum ($b/a= 0,90$)	3,020	3,043	6,226	6,283
Aluminum ($b/a= 0,95$)	3,043	3,057	6,262	6,273
Copper ($b/a= 0,93$)	2,278	2,297	4,572	4,588
Copper ($b/a= 0,94$)	2,289	2,309	4,578	4,607

Finally, Young's modulus and Poisson's ratio of aluminum and copper are determined, using Eq. (9) and Eq. (10). Estimated values are presented in Table III.

Table III: Estimated Young's modulus (GPa) and Poisson's ratio of aluminum and copper.

	Spectrogram		Concentrated Spectrogram		Experiment	
	E	ν_p	E	ν_p	E	ν_p
Aluminum ($b/a= 0,90$)	69,8	0,347	68,8	0,346	69,0	0,340
Aluminum ($b/a= 0,95$)	69,8	0,345	70,3	0,344	69,0	0,340
Copper ($b/a= 0,93$)	125,4	0,334	123,6	0,332	124,0	0,330
Copper ($b/a= 0,94$)	126,7	0,333	124,6	0,332	124,0	0,330

Briefly exploring the results in Table III, we have shown that Spectrogram and Concentrated Spectrogram representations are advantageous. Mechanical parameters of aluminum and copper such as Young's modulus and Poisson's ratio are calculated with good precision (less than 1 %).

VI. CONCLUSION

In this paper, we have demonstrated that the study of acoustic signals backscattered by air-filled one-layer cylindrical tubes, immersed in water, provides the mechanical properties (Young's modulus and Poisson's ratio) of homogeneous solid materials. The analysis of time-frequency images, toward normalized frequencies ranging from 0.1 to 500, shows the guided waves propagation. Reduced cutoff frequencies of A_1 and S_1 waves are extracted from Spectrogram and concentrated Spectrogram time-frequency images. Young's modulus and Poisson's ratio of aluminum and copper are estimated accurately.

REFERENCES

[1] Jiangong Yu, J. E. Lefebvre, L. Elmaïmouni, "Toroidal wave in multilayered spherical curved plates," *Journal Sound and Vibration* **332**, 2816-2830, 2013.

[2] J. Jamali, M. H. Naet, F. Honarvar, M. Rajabi, Acoustic scattering from functionally graded cylindrical shells, *Arch. Mech. Warszawa*, **63** (1), 25-56, 2011.

[3] Liang-Wu Cai, J. Sánchez Dehesa, Acoustic scattering by radially stratified scatterers, *Journal of the Acoustical Society of America* **124**, 2715-2726, 2008.

[4] F. Chati, F. Léon, G. Maze, Acoustic scattering by a metallic tube with a concentric solid polymer cylinder coupled by a thin water layer. Influence of the thickness of the water layer on the two Scholte-Stoneley waves, *Journal of the Acoustical Society of America* **118**, 2820-2828, 2005.

[5] G. Maze, F. Léon, J. Ripoché, A. Klauson, J. Metsaveer, H. Überall, Nature de l'onde de Scholte sur une coque cylindrique, (Nature of the Scholte wave on a cylindrical shell), *Acustica, International Journal on Acoustics* **81**, 201-213, 1995.

[6] A. Mal, and S.-S. Lih, Characterization of the elastic properties of composite interfaces by ultrasonic nde. In D.O. Thompson and D.E.

Chimenti, editors, *Review of Progress in Quantitative NDE*. Plenum Press, New York, 1992.

[7] D.N. Alleyne, and P. Cawley, Optimization of Lamb wave inspection techniques, *NDT E. Int.* **25**, 11-22, 1992.

[8] A.H. Nayfeh, and D.E. Chimenti, Propagation of guided waves in fluid-coupled plates of fibre-reinforced composite, *J. Acoust. Soc. Am.*, **83**: 1736-1743, 1988.

[9] G. Maze, J.-L. Izbicki, Jean Ripoché, Acoustic scattering from cylindrical shells: guided waves and resonances of the liquid column, *Ultrasonics* **24**, 354-361, 1986.

[10] G. Maze, J.-L. Izbicki, J. Ripoché, Resonances of plates and cylinders: Guided waves, *Journal of the Acoustical Society of America* **77**, 1352-1357, 1985.

[11] L. Flax, V. K. Varadan, and V. V. Varadan, "Scattering of an obliquely incident wave by an infinite cylinder," *J. Acoust. Soc. Am.* **68**, 1832-1835, 1980.

[12] P. Flandrin, "Temps-Fréquence," Hermès, Paris, 7-390, 1993.

[13] L. Cohen, "Time-Frequency Analysis," Prentice Hall, PTR, the City University of New York, 1-316, 1995.

[14] L. Cohen, "Time-frequency distribution—a review," *Proc IEEE*, **77**(7), 941-981, 1989.

[15] P.Flandrin, F.Auger, E.Chassande-Mottin, "Time-frequency reassignment: From principles to algorithms, Applications in Time-Frequency Signal Processing," CRC Press, 179-203, 2003.

[16] K. Fitz, L. Haken, "On the use of time-frequency reassignment in additive sound modeling", *J. Audio Eng. Soc.* **50**, 879-893, 2002.

[17] S.W. Hainsworth, M.D. Macleod, "Time-frequency reassignment: a review and analysis," *Tech. Rep. CUED/FINFENG/TR*, **459**, Cambridge University, Engineering Department, 2-27, 2003.

[18] D.J. Nelson, "Cross-Spectral Methods for Processing Speech," *J. Acoust. Soc. Am.* **110**, 2575-2592, 2001.

[19] B.A. Auld, *Acoustic Fields and Waves in Solids*, Volume **1**, Krieger Publishing Company Malabar, Florida, 1990.

[20] J. Lefebvre, P. Lasaygue, C. Potel, J. Belleval and P. Gatignol, L'acoustique ultrasonore et ses applications, 1^{ère} partie Acoustique et Techniques N° 36, 8723, 4-11, 2004.

[21] D. Royer and E. Dieulesaint, *Ondes élastiques dans les solides*, Tome 1, Masson et Cie, Paris, 2000.